For Article (Discoveries)

Title: Gene expression does not support the developmental hourglass model in three animals with spiralian development

Authors:

Longjun Wu* (longjunwu@rochester.edu)

Kailey E. Ferger (kferger@u.rochester.edu)

J. David Lambert* (dlamber2@mail.rochester.edu)

* co-corresponding authors

Author affiliations

Department of Biology, University of Rochester, Rochester, NY 14627, USA

Contact info

Correspondence:

dlamber2@mail.rochester.edu

longjunwu@rochester.edu

Abstract

It has been proposed that animals have a pattern of developmental evolution resembling an hourglass because the most conserved development stage—often called the phylotypic stage—is always in mid-embryonic development. Although the topic has been debated for decades, recent studies using molecular data such as RNA-seq gene expression datasets have largely supported the existence of periods of relative evolutionary conservation in mid-development, consistent with the phylotypic stage and the hourglass concepts. However, so far this approach has only been applied to a limited number of taxa across the tree of life. Here, using established phylotranscriptomic approaches, we found a surprising reverse hourglass pattern in two molluscs and a polychaete annelid, representatives of the Spiralia, an understudied group that contains a large fraction of metazoan body plan diversity. These results suggest that spiralians have a divergent mid-embryonic stage, with more conserved early and late development, which is the inverse of the pattern seen in almost all other organisms where these phylotranscriptomic approaches have been reported. We discuss our findings in light of proposed reasons for the phylotypic stage and hourglass model in other systems.

Introduction

Nearly two hundred years ago, von Baer reported the striking morphological similarity of early embryos within the vertebrates (Von Baer, 1828). Subsequent observations showed that the earliest embryonic development stages are morphologically variable, followed by a mid-embryonic stage with morphological similarity reaching maximum levels, progressing to later stages showing increased morphological divergence (Duboule, 1994; Raff, 1996; Slack et al., 1993). This developmental pattern was later termed the "hourglass", because a visual representation of the variability present throughout developmental ontology would have the shape of an hourglass, with the constricted waist at the most conserved mid-embryonic stage; this conserved stage was termed the phylotypic stage (Sander, 1983).

Historically, however, this model has been controversial; debate on the existence of the hourglass pattern and phylotypic stages in various groups has been ongoing for decades (Richardson 1995; Hall 1997; Richardson et al. 1997; Collazo 2000; Bininda-Emonds et al. 2003). Its major criticism focused on the definition of the most conserved stage, or phylotypic stage, on the grounds that the model is based on morphological similarity, a subjective anatomical comparison. Remarkably, this controversy seems to have quieted in recent years due to the application of new and potentially more objective quantitative molecular/genomics approaches. Recent studies in multiple taxa, based on measurements of the evolutionary age or rate of genes that are expressed at different developmental stages, nearly unanimously report a more conserved and evolutionarily older mid-embryonic stage and thus support the existence of a phylotypic stage and the hourglass model (reviewed in Drost et al. 2017).

One approach that has been used to compare the relative evolutionary age of developmental stages is called phylotranscriptomics (Domazet-Lošo and Tautz 2010). In this method, genes of an organism are first assigned to different age categories, based on how broadly they are conserved in a phylogeny. This measurement is combined with gene expression data to compute a weighted transcriptome age index (TAI) of each developmental stage. A lower TAI indicates relatively higher expression of older genes and

lower expression of younger genes during this stage; thus, the stage with lower TAI is considered more conserved compared to other stages. Such studies have generally reported that the lowest TAI, or most conserved stage, is in mid-embryogenesis, while a higher TAI was found in earlier and later stages (Domazet-Lošo and Tautz 2010; Drost et al. 2015; Xu et al. 2016; reviewed in Drost et al. 2017). In these cases, the lowest TAI stage often coincides with the proposed phylotypic stage of that phylum, supporting the existence of the phylotypic stage and the hourglass model. While most of these studies have demonstrated an hourglass model, in several others a pattern of early embryonic conservation of gene expression patterns has been reported (Piasecka et al. 2013; Liu and Robinson-Rechavi 2018).

The hourglass pattern has been found outside of animals, in fungi (Cheng et al. 2015) and plants (Quint et al. 2012). The phylogenetic breadth of the organisms where this pattern has been found has led to the suggestion that this is a fundamental characteristic of the ontology of multicellular organisms (Cheng et al. 2015). In addition, the pattern has recently been reported in biological processes other than developmental ontology, such as organogenesis (Drost et al. 2016) and stress responses (Durrant et al. 2017). The apparent ubiquity of the hourglass pattern has leaded to the hypothesis that this pattern is not just a characteristic of developmental ontology, but a general pattern of evolution for complex biological processes (Drost el al. 2016, 2017).

To date, only a scattered sampling of organisms in the tree of life have been studied using this approach. For example, studies of the developmental phylotranscriptomics in plant and fungi both have only been reported from one species (Quint et al. 2012; Cheng et al. 2015). Similarly, most animal studies focus on Deuterostomia and Ecdysozoa, two clades of Bilateria, while Spiralia, the other major bilaterian group, has rarely been examined.

Spiralia is an ancient and highly diverse clade of protostome animal groups. It contains about 11 of the 25 extant bilaterian phylum-level groups, including molluscs, annelids, brachipods, phoronids, nemerteans, bryozoans, rotifers and platyhelminthe flatworms (Fig.1A; Giribet et al. 2000; Dunn et al, 2008; Hejnol 2010; Laumer et al. 2015).

The adult body plans of spiralians are extremely diverse, but there are two developmental stages that might arguably be considered phylotypic stages. The first is the spiral cleavage program in early development, which inspired the name Spiralia when it was recognized as homologous between molluscs, annelids and flatworms (Schleip 1929). This cleavage pattern is characterized by highly regular asymmetries and cleavage angles during early divisions (Fig. 1B). It is also associated with strong similarities in the fate map of the blastula produced by these divisions. For instance, precisely the same cell in the lineage generates endomesoderm in all groups with spiral cleavage (reviewed in Lambert 2008). Since Schleip, the conserved spiral cleavage has also been recognized in nemerteans, and modified spiral cleavage has possibly been detected in other groups of spiralians (reviewed in Hejnol 2010; Lambert 2010; Vellutini et al 2017). This level of conservation within and between phylum-level groups in cleavage pattern and early cell fate specification is unparalleled across the animal kingdom.

The other candidate for a phylotypic stage is the distinctive trochophore larva, found in molluscs and annelids (Fig. 1C) (Maslakova et al. 2004; Nielsen 2004, 2005; Raff 2008). This pelagic larva has a pre-oral circumferential ciliary band that is used for feeding and swimming, an apical tuft of cilia at the anterior end, and a posterior ring of cilia called the telotroch. The trochophore larva stage generally occurs while organogenesis is ongoing, and the basic bodyplan is emerging. The trochophore stage has in fact been proposed to be the phylotypic stage for molluscs and annelids (Cohen and Massey 1983; Slack 2003; Shigeno et al. 2010; Levin et al. 2016).

Compared to the other two clades of bilaterian animals, there are fewer spiralian model systems and less genomic data available for these animals. One recent paper recovered the hourglass pattern from spiralian transcriptomic datasets (Xu et al. 2016), and has been widely cited as evidence of the hourglass model in spiralian development (Irie 2017; Drost et al. 2017; Hu et al. 2017; Uchida et al. 2018). Here we revisit this question using a refined calculation method and recently accumulated spiralian genomic and transcriptomic data, and find that spiralian development does not follow the predictions of the hourglass model, but instead shows a striking reverse hourglass pattern. Our results

show that in spiralians, one of the previously proposed phylotypic stages—the trochophore, is the least conserved in terms of the evolution of expressed genes. This work highlights the uniqueness of spiralian development and adds important refinements to phylotranscriptomics approach.

Results

TAI profiles of oyster C. gigas *development show a reverse hourglass pattern*

To explore the relative ages of genes expressed at different developmental stages in a spiralian, we started by calculating the TAI of a bivalve mollusc, the pacific oyster *Crassostrea gigas*. This species has extensive genomic resources, including a well-assembled and annotated genome, and a comprehensive transcriptome data set of developmental stages (Zhang et al. 2012). In addition, *C. gigas* has typical spiralian development with spiral cleavage in early development and the conserved trochophore larva in the mid-embryogenesis stage—the proposed phylotypic stage of molluscs and annelids. Finally, the taxonomic lineage leading to *C. gigas* (Mollusca, Bivalvia, Pteriomorphia, Ostreoida, Ostreidae, Crassostrea) is one of the most comprehensively studied in spiralians in terms of the availability of genomic and transcriptomic data, which should improve the resolution of *C. gigas*'s gene age assignment in TAI studies.

We computed the TAI of *C. gigas* using standard approaches (Domazet-Lošo et al. 2007; Domazet-Lošo and Tautz 2010; see Methods for details). Briefly, we first organized the *C. gigas* genes into 14 age levels, termed phylostrata, based on BLAST searches against comprehensive databases. The phylostrata is defined as the oldest phylogenetic node where a gene has detectable orthologs, and it represents the gene's age in a hierarchical taxonomic order in the tree of life. We then determined the TAI value of each developmental stage based on relative expression of genes from different phylostrata using transcriptomic data (see Methods for details). As shown in Fig. 2A, the TAI profile of *C. gigas* development has a prominent peak during the trochophore stage, roughly in the middle of the developmental sequence, showing a reverse hourglass pattern. This indicates that this stage has relatively high expression of younger genes and is thus less conserved than earlier and later stages by this measure. This pattern directly opposes suggestions that the trochophore stage is the phylotypic stage of spiralians based on morphology (Cohen and Massey 1983; Slack 2003; Shigeno et al. 2010) and the previous assessment of the TAI pattern in this species (Xu et al. 2016). It is also contrary to a study arguing support of the hourglass model based on the expression patterns of novel homeobox genes in this group (Paps et al.

159 2015).

160 We followed most other previous TAI studies based on transcriptomic sequencing
161 data by normalizing the data (TPM normalization) but not transforming it. Two recent
162 studies show that square root or log transformation of the expression data can change the
163 observed pattern (Piasecki et al. 2013; Liu and Robinson-Rechavi 2018). We performed
164 square root transformation to our TAI result and it still shows a significant peak at the
165 trochophore stage, but it is less prominent compared to the pattern calculated by the
166 untransformed data (compare Fig. S1 with Fig. 2A); this seems to be caused by relatively
167 higher TAI values after the trochophore stage. Thus, under this transformation, the data is
168 also consistent with an "early conservation" pattern, but it is still not consistent with the
169 typical hourglass pattern.

170 The previous report of the TAI profile of *C. gigas* development found that the
171 trochophore stage was enriched for young genes, and they recovered an hourglass pattern
172 only after the removal of such genes from the analysis (Xu et al. 2016). Their study was
173 performed when only a few spiralian genomes and transcriptomes were available, thus the
174 taxonomic resolution was low; for example, only three phylostrata younger than Spiralia
175 were used: Mollusca, Bivalvia and *C. gigas*. We wondered whether inclusion of more data
176 would show that some of the genes that were considered species-specific are actually in
177 older phylostrata. Indeed, in our study, with a more comprehensive spiralian database, there
178 is better taxonomic resolution in spiralians and far fewer genes assigned to the species-
179 specific category (Fig 2B, 996 vs. 3448). To test if our reverse hourglass TAI profile is
180 robust after removing younger genes, we computed TAI profiles for *C. gigas* with
181 progressively older phylostrata removed, starting with a profile after the species-specific
182 genes were removed (Fig. 2B). In contrast to the previous study, the reverse hourglass
183 pattern we observed persists even after removing all phylostrata younger than Bivalvia.
184 When the reverse hourglass pattern does disappear, the remaining TAI profile is generally
185 flat—there is no other large peak or trough in the pattern. This result is conservative
186 because with more spiralian genomic data added in the future, more genes will be assigned
187 to older phylostrata. In sum, the reverse hourglass pattern found in *C. gigas* is not just

188 derived from species-specific genes, but is instead a general pattern that is driven by many
189 other genes from multiple phylostrata.

190 The reverse hourglass may have been caused by abnormal development of
191 experimental subject animals or experimental errors during production or assembly of the
192 transcriptome data. To address this concern, we performed an additional TAI calculation
193 based on a recently published experimental replicate of *C. gigas* transcriptome data
194 sequencing, which covers major stages over the entire ontology (Xu et al. 2016). As shown
195 in Fig. 2C, the TAI profile of this replicated experiment shows a similar result to our first
196 set of experimental data, with the highest TAI in the trochophore stage. Thus, this pattern
197 is unlikely to be caused by experimental variation.

198 A difference in the computation of TAI also contributed to the discrepancy between
199 our results and those of Xu et al. (2016). TAI is calculated as the phylostrata-weighted sum
200 of gene expression divided by the sum of unweighted gene expression. Like other previous
201 analyses, when they computed the TAI after younger phylostrata were removed, they only
202 deducted the weighted sum of gene expression of that phylostrata (from the numerator) and
203 did not remove the sum of gene expression of that phylostrata (from the denominator)
204 (Domazet-Lošo and Tautz 2010; Cheng et al. 2015; Xu et al. 2016; Drost et al. 2018). While
205 this may be suitable to show the contribution of each phylostrata to the overall TAI pattern,
206 it is not appropriate for studying the developmental TAI profile after certain phylostrata are
207 removed because it will systematically bias the results, in some cases reversing the pattern.
208 For instance, if the TAI of the peak stage was largely contributed by younger phylostrata,
209 when only removing the weighted sum of gene expression from these younger phylostrata
210 from the numerator, the TAI of the peak stage will be reduced to the lowest. This is because
211 the sum of the gene expression (the denominator) of the peak stage represents the largest
212 of all stages, as this stage has the highest expression of those younger phylostrata. This
213 largest sum's inclusion in the denominator makes this peak stage's TAI the smallest TAI
214 value of all stages, which inverts the overall TAI pattern. This explains why they reported
215 a reverse hourglass for the overall pattern, but an hourglass pattern after removing the
216 younger genes. In our study, we removed gene expression from both the numerator and the

denominator when we removed successive phylostrata; this resulted in a reverse-hourglass model even after removal of phylostrata younger than Bivalvia (see Methods for details). When we employed the calculation method from other previous analyses for our data, we observed the hourglass pattern after removing phylostrata younger than Mollusc (Fig. 3A); on the other hand, when the new calculation method presented here was used for the data generated by Xu et al. (2016), the hourglass pattern disappeared (Fig. 3B).

The TDI profile also supports the reverse hourglass model

Another method to measure relative conservation of developmental stages is to compare the expression of conserved and fast-evolving genes. This approach generates what is called the transcriptome divergence index (TDI; Quint et al. 2012). Compared to TAI analysis, which assigns genes to different phylostrata, the TDI uses the sequence divergence of genes to represent the evolutionary conservation of a gene. As with the TAI, the distance is weighted by gene expression. A higher TDI value indicates higher expression of fast-evolving genes, or less evolutionary constraint within a stage. TDI reflects the selection pressure on the development stage. Using another oyster in the same genus, *C. virginica* (Gómez-Chiarri et al. 2015), we calculated the *C. gigas*' gene conservation level by comparing orthologous gene pairs of these two species (Drost et al. 2018). As shown in Fig. 4, the TDI profile shows a strong similarity to the profile created using the TAI method, with the highest TDI value in the trochophore stage. Since TDI also indicates whether the observed pattern is actively maintained (Drost et al. 2015), the TDI result also shows that this pattern was preserved at least after the splitting between *C. gigas* and *C. virginica.*

The TAI profiles of two other spiralians also show reverse hourglass pattern

To determine if the reverse hourglass pattern is restricted to *C. gigas*, we performed TAI studies in the mollusc *Haliotis discus hannai* and the annelid *Perinereis aibuhitensis*. Annelids are allied with molluscs in the Spiralian subclade Lophotrochozoa; their common ancestor dates back to at least the Cambrian, more than 500MYA. The TAI profile of the abalone *H. discus* is low at the earliest stage, and generally much higher for the rest

of the profile, with the peak value at the trochophore stage (Fig. 5A). Thus, the profile for this species generally resembles a reverse hourglass but it is less pronounced than for the *C. gigas*; the profile definitely does not resemble an hourglass pattern. The profile of the annelid *P. aibuhitensis* strongly resembles the reverse hourglass figure seen in the oyster *C. gigas*, with the peak TAI also at the trochophore stage. These findings indicate that the reverse hourglass pattern is not restricted to oyster *C. gigas* and may be conserved in other spiralians.

Discussion

Here we report a reverse hourglass pattern in spiralian development using phylo-transcriptomic approaches in two species of molluscs and one annelid. In the oyster *C. gigas,* this pattern remains robust after removing genes from younger phylostrata as well as when using an experimental replicate dataset. Our results indicate that, contrary to earlier conclusions based on comparative morphology (Cohen and Massey 1983; Slack 2003; Shigeno et al. 2010) and molecular approaches (Xu et al. 2016; Paps et al. 2015), *C. gigas* has a divergent mid-embryonic (trochophore) stage, with more conserved early and late development. This result seems to be true for another mollusc and an annelid.

The reverse hourglass pattern we observed implies that there is no one stage of the three spiralians' development that is particularly constrained, and in fact, the trochophore stage midway through development is relatively fast-evolving. The trochophore stage occurs during organogenesis in spiralians. It has been argued that phylotypic stages in other taxa occur during organogenesis because different organ systems have to coordinate development resulting in a complex pattern of interactions (Raff 1996). It is possible that spiralian organogenesis is less integrated than in other clades. Classically, spiralian development was considered to be more reliant on autonomous patterning mechanisms, resulting in a "cleavage mosaic" of largely independently developing lineages (Wilson 1904). Given this view, it could be argued that the apparent lack of constraint during spiralian organogenesis reflects a lack of signalling between clones that are making different organs. However, the available evidence suggest that cell signalling is important in spiralian embryos, indicating that lineages are not independently developing in organogenesis. Cases of signalling and regulation during organogenesis are known (Cather et al. 1967; Chan and Lambert 2011), and several organs are formed from combinations of cells from different clones, which likely requires communication between cell populations (e.g. heart, mouth, shell; Chan and Lambert 2014). Thus, we would expect that the developmental integration of various lineages in spiralian organogenesis is similar to other taxa, and unlikely to explain the reverse hourglass pattern.

In other groups, the Hox genes are patterning the embryo during the phylotypic stage, and regulatory interactions between these genes have been invoked to explain the hourglass model (Duboule 1994). In the oyster *C. gigas*, the Hox genes are not preferentially expressed during the trochophore stage (see Fig. S18 in Zhang et al. 2012). Overall, three Hox genes have peak expression earlier than the trochophore stage, two have peak expression in the trochophore, and five have peak expression after. Thus, the trochophore stage does not appear to be a particularly important stage for Hox gene patterning.

It may be that the pattern we observe is caused by more specific processes that are occurring in the trochophore stage. In fact, some key spiralian and molluscan synapomorphies are developing at this time. *Ectomesoderm* is a spiralian-specific form of mesoderm that is proliferating and forming body muscles at this stage, so genes that are specifically associated with ectomesoderm could contribute to the pattern. The trochophore is named after the primary ciliary band of the larva, the *prototroch*. This structure appears near the beginning of trochophore stage, and is elaborated progressively in the groups considered here. If ciliary band genes are relatively young and fast-evolving, they could also be contributing. The shell is a molluscan synapomorphy which starts to develop shortly before the trochophore stage. Intriguingly, biomineralization proteins that control shell deposition are enriched for fast-evolving and novel genes (Aguilera et al. 2017), providing a potential explanation for the reverse hourglass. However, shell growth continues after the trochophore stage when the peak is observed, and the biomineralization genes would be expected to be expressed continuously with shell growth; in fact, the relative size of the shell forming tissue increases over time, in contrast to the drop in young and fast evolving genes. Moreover, the reverse hourglass was also observed in the polychaete annelid, which does not have a shell.

There are potential ecological explanations for the pattern we observe (Kalinka and Tomancak 2010). The trochophore stage is just after hatching from the egg membrane, when the organism first makes direct contact with the seawater. This raises the possibility that the peak we see is driven by young and fast-evolving genes that are involved in

adaptation to aspects of the marine environment. However, it is not clear why this stage should respond differently to the environment than other pre-metamorphic stages that follow it.

Finally, another general explanation for the pattern we observe is that the earlier and later stages are relatively conserved because of negative selection (Zalts and Yanai 2017). Early spiralian development is famously conserved, and thus might be under particularly strong purifying selection. In contrast, the post-trochophore stages are when the body plan is being elaborated, and it is not clear why these would be subject to stronger negative selection than the trochophore stage.

In sum, it seems that current explanations of the evolutionary forces that may drive the hourglass pattern are not sufficient to explain the pattern we observed here. Our results also show that conclusively establishing patterns across the tree of life requires some level of sub-sampling within high-level groups, along with broad sampling across these groups. The Spiralia is a large, diverse and disparate group that contains a significant fraction of the body plan diversity in the Metazoa. Inclusion of multiple spiralian taxa in any survey of animal development is essential to capture the true diversity of animals. Finally, given the newly apparent diversity in the patterns of developmental conservation in bilaterians, it would be very interesting to examine the pattern in an outgroup, such as a cnidarian.

Materials and Methods

We followed standard methods for calculating TAI (Domazet-Lošo et al. 2007; Domazet-Lošo et al. 2010). To assign genes into phylostrata, each *C. gigas*, *H. discus hannai* and *P. aibuhitensis* gene was first BLASTp (BLAST v. 2.7.1+) searched against the NCBI nr database (downloaded March, 2018) with an e-value cut-off of 0.00001. Employing the "staxids" option in the BLASTp search, the taxonomic ID of hits were returned. The taxonomic ID was then used to extract taxonomic information from the NCBI taxonomic file "gi_taxid_prot.dmp.gz", downloaded from ftp://ftp.ncbi.nlm.nih.gov/pub/taxonomy/. Note that because the spiralian phylum Platyhelminthes (flatworm) is not listed as a spiralian clade in NCBI's taxonomic information, we adjusted their taxonomic information accordingly. Since spiralian sequences are relatively rare in NCBI database, we also supplement the sequence collection by building a spiralian genome database and a spiralian transcriptome database manually, which include 14 and 7 species respectively (Supplemental table 1). These databases were specifically enriched for the taxonomic lineage leading to *C. gigas*. BLASTp and BLASTx were then performed to search against these two databases respectively.

The phylostrata analysis for TAI

The BLAST search and processing of the results were performed by an inhouse python script (https://github.com/longjunwu/Genomic-phylostratigraphy-tool). As in previous studies (Domazet-Lošo et al. 2007) we discarded hits to non-cellular organisms and organisms of uncertain taxonomic status (environmental, uncultured samples). Each gene was then assigned to one of the 14 phylostrata according to the hit to the deepest phylogenetic level. If no homology was found, the gene was considered as orphan gene and assigned to the highest (youngest, or species-specific) phylostrata. The phylostrata of gene analysed are included in Supplemental Table 2.

There is ongoing debate about the biases that can be caused by using BLAST to determine gene age (Moyers and Zhang 2015, 2017, 2018; Domazet-Lošo et al. 2017; Yin et al. 2018; Casola 2018). The most marked of these potential biases are caused by short

genes, and fast evolving genes, both of which are more likely to be assigned to younger phylostrata by BLAST (Moyers and Zhang 2015). In general, even if some genes are assigned incorrectly, using BLAST to determine phylostrata should not have serious effects on TAI profiles because the phylostrata assigned are identical across all stages and the TAI profiles are based on the relative value of transcriptomic age index across stages, not the absolute transcriptomic index value of the stages. Thus, BLAST bias of phylostrata assignment, if exist, is likely uniform across the stages. Unless, for instance, the pattern we observe here is caused by disproportionate numbers of short and/or fast evolving genes in the trochophore stages. If these were incorrectly assigned to young phylostrata, it could cause the TAI peak we observe. We checked this by plotting the gene length normalized by expression levels (transcriptomic length index) across stages (Fig. S3). The curve was generally noisy but flat and the trochophore stage had typical values, indicating that gene length is unlikely to be biasing our result.

According to previous study, the shortest and fastest-evolving genes are most likely to be causing BLAST biases (Moyers and Zhang 2015). To see if such bias was causing the pattern we observe, we calculated the TAI after removing the top 30% shortest genes (Fig. S4A), or after removing the top 30% fastest-evolving genes (Fig. S4B). The reverse hourglass TAI is still significant in both of these tests. Taken together, this evidence shows that the reverse-hourglass pattern we observed is unlikely to be caused by BLAST bias.

The dN/dS analysis for TDI

A gene divergence map (dN/dS) between the CDS of *C. gigas* and C. *virginica* genome was calculated with default setting using an R package "orthologr" developed by Drost et al. (2015). These are the only two genome assemblies from the *Crassostrea* genus we have access to. The dN/dS estimation methods we used was "NG": Nei, M. and Gojobori, T. (1986). The dN/dS and dS of gene analysed are included in Supplemental Table 3.

If a pair of species used to calculate dNdS are too divergent, the dS could be saturated, which would affect the estimation of dN/dS. To address this concern, we calculated the distribution of dNdS (Fig. S5) and dS (Fig. S6). Our result shows that most

genes have dS smaller than 3, an dS saturation cut off suggested by Yang (2014), but a few are higher.

Even if the dS is saturated for some genes, if the degree of potential saturation is uniform across the developmental stages, it should not seriously affect the TDI profile. We checked this by plotting the dS normalized by expression levels (transcriptomic synonymous index) across stages (Fig. S7). The curve was generally noisy but the trend was flat and the trochophore stage had typical values, indicating that saturation of dS, if exist, is unlikely to be biasing our result. To further rule out the possibility of the effects to TAI profile caused by the bias of saturated dS, we removed genes with dS larger than 1 and then calculated the TDI. The TDI after removing these genes still shows a significant reverse hourglass pattern (Fig. S8), indicating that it is not just genes with saturated dS that contribute to the pattern.

To test the robustness of the results from different dN/dS estimation methods, we also employed three additional models included in the "orthologr" package: "LPB": Li, W.H. (1993) and Pamilo, P. and Bianchi, N.O. (1993); "MYN": Zhang, Z., et al. (2006) and "GY": Goldman, N. and Yang, Z. (1994). The results from these models are shown in Fig. S9. They show similar reverse hourglass patterns, indicating that the reverse hourglass result is not sensitive to the model used.

Gene expression profiles

The raw reads from the transcriptome sequencing of the developmental stages of *C. gigas* were acquired from Zhang et al. (2012). The data from the transcriptome sequencing of the developmental stages of *H. discus hannai*, *P. aibuhitensis* and replicated *C. gigas* were acquired from Xu et al. (2016). The R package RSEM (Li and Dewey 2011) was used to align raw reads to the reference genome of *C. gigas*, and reference transcriptome of *H. discus hannai* and *P. aibuhitensis* (Zhang et al. 2012; Xu et al. 2016). The command "rsem-calculate-expression" was employed to calculate the gene expression with default settings. The TPM (Transcripts Per Kilobase Million, Wagner et al. 2012) normalized count was used as the expression read count (expression level). All genes annotated in the *C. gigas*

assembly were included in the following analysis. The expression levels of all genes are included in Supplemental Table 2

Finally, we calculated the TAI and TDI for each stage using the following equations: $TAI\_s = \frac{\sum_{i=1}^{n} PS_i E_{i\_s}}{\sum_{i=1}^{n} E_{i\_s}}$, $TDI\_s = \frac{\sum_{i=1}^{n} D_i E_{i\_s}}{\sum_{i=1}^{n} E_{i\_s}}$, where PS_i represents the phylostratum of the gene i, E_{i_s} represents the expression level of each gene at stage s, n is the total number of genes analyzed, and D_i represents dN/dS value calculated from the "orthologr" package (Drost et al. 2015).

The TAI formula can also be written as $TAI\_s = PS_1 * \frac{E_{1\_s}}{E_{1\_s}+E_{2\_s}+\cdots+E_{n\_s}} + PS_2 * \frac{E_{2\_s}}{E_{1\_s}+E_{2\_s}+\cdots+E_{n\_s}} + \ldots + PS_n * \frac{E_{n\_s}}{E_{1\_s}+E_{2\_s}+\cdots+E_{n\_s}}$ where PS_i represents phylostratum, E_{n_s} is the sum of gene expression of a given phylostratum at stage s, and n is the total number of phylostratum analyzed. For the calculation of TAI when genes from younger phylostrata were removed, these genes from that specific phylostrata were excluded from both the numerator and the denominator of the equation: $TAI\_s = PS_1 * \frac{E_{1\_s}}{E_{1\_s}+E_{2\_s}+\cdots+E_{(n-1)\_s}} + PS_2 * \frac{E_{2\_s}}{E_{1\_s}+E_{2\_s}+\cdots+E_{(n-1)\_s}} + \ldots + PS_{n-1} * \frac{E_{(n-1)s}}{E_{1\_s}+E_{2\_s}+\cdots+E_{(n-1)s}}$. To show the results from the calculation used in previous studies (Domazet-Lošo and Tautz 2010; Cheng et al. 2015; Xu et al. 2016; Drost et al. 2018), the genes from that specific younger phylostrata were only excluded from numerator of the equation: $TAI\_s = PS_1 * \frac{E_{1\_s}}{E_{1\_s}+E_{2\_s}+\cdots+E_{n\_s}} + PS_2 * \frac{E_{2\_s}}{E_{1\_s}+E_{2\_s}+\cdots+E_{n\_s}} + \ldots + PS_{n-1} * \frac{E_{(n-1)s}}{E_{1\_s}+E_{2\_s}+\cdots+E_{n\_s}}$.

The standard deviation of the TAI/TDI profiles, the significance tests of the reverse hourglass patterns and significance tests of flatline pattern were estimated using permutation analysis by the "PlotSignature", "ReverseHourglassTest" and "FlatLineTest" functions, respectively, in the myTAI package (Drost et al., 2018).

Acknowledgement

The authors thank Dr. Hajk-Georg Drost for implementing "ReverseHourglassTest" function in myTAI package, the Steven Roberts lab for their early sharing of the *Ostrea lurida* genome data, the *Crassostrea virginica* genome sequencing group for their early sharing of the *C. virginica* genome data and Dr. K. Tu for early sharing of the transcriptome data of *Crassostrea hongkongensis*. This work was supported by two grants by the National Science Foundation to J.D.L. (grant number IOS-1146782 and IOS-1656558).

444 **References**

445 Aguilera F, McDougall C, Degnan BM. 2017. Co-option and de novo gene evolution
446 underlie molluscan shell diversity. *Mol Biol Evol*. 34:779-792.

447 Bininda-Emonds OR, Jeffery JE, Richardson MK. 2003. Inverting the hourglass:
448 quantitative evidence against the phylotypic stage in vertebrate development. *Proc. Royal*
449 *Soc. Lond. Series B: Biological Sciences.* 270:341-346.

450 Casola C. 2018. From De Novo to "De Nono": The Majority of Novel Protein-Coding
451 Genes Identified with Phylostratigraphy Are Old Genes or Recent Duplicates. *Genome Biol*
452 *Evol.* 10:2906-2918.

453 Cather JN. 1967. Cellular interactions in the development of the shell gland of the
454 gastropod, Ilyanassa. *J Exp Zool.* 166:205-223.

455 Chan XY, Lambert JD. 2011. Patterning a spiralian embryo: a segregated RNA for a Tis11
456 ortholog is required in the 3a and 3b cells of the Ilyanassa embryo. *Dev Biol.* 349:102-112.

457 Chan XY, Lambert JD. 2014. Development of blastomere clones in the Ilyanassa embryo:
458 transformation of the spiralian blastula into the larval body plan. *Dev Genes Evol*. 224:159-
459 174.

460 Cheng X, Hui JH, Lee YY, Wan Law PT, Kwan HS. 2015. A "developmental hourglass" in
461 fungi. *Mol Biol Evol*. 32:1556-1566.

462 Cohen J, Massey BD. 1983. Larvae and the origins of major phyla. *Biol J Linnean Soc.*
463 19:321-328.

464 Collazo A. 2000. Developmental variation, homology, and the pharyngula stage. *Syst Biol*.
465 49:3-18.Domazet-Lošo T, Brajković J, Tautz D. 2007. A phylostratigraphy approach to
466 uncover the genomic history of major adaptations in metazoan lineages. *Trends Genet*.
467 23:533-539.

468 Domazet-Lošo T, Tautz D. 2010. A phylogenetically based transcriptome age index mirrors
469 ontogenetic divergence patterns. *Nature.* 468:815.

Domazet-Lošo T, Carvunis AR, Albà MM, Šestak MS, Bakaric R, Neme R, Tautz D. 2017. No evidence for phylostratigraphic bias impacting inferences on patterns of gene emergence and evolution. *Mol Biol Evol*. 34:843-856.

Drost HG, Gabel A, Grosse I, Quint M. 2015. Evidence for active maintenance of phylotranscriptomic hourglass patterns in animal and plant embryogenesis. *Mol Biol Evol.* 32:1221-1231.

Drost HG, Bellstädt J, Ó'Maoiléidigh DS, Silva AT, Gabel A, Weinholdt C, Ryan PT, Dekkers BJ, Bentsink L, Hilhorst HW, et al. 2016. Post-embryonic hourglass patterns mark ontogenetic transitions in plant development. *Mol Biol Evol.* 33:1158-1163.

Drost HG, Gabel A, Liu J, Quint M, Grosse I. 2018. myTAI: evolutionary transcriptomics with R. *Bioinformatics.* 34:1589-1590.

Drost HG, Janitza P, Grosse I, Quint M. 2017. Cross-kingdom comparison of the developmental hourglass. *Curr Opin Genet Dev.* 45:69-75.

Duboule D. 1994. Temporal colinearity and the phylotypic progression: a basis for the stability of a vertebrate Bauplan and the evolution of morphologies through heterochrony. *Dev Suppl*. 1994:135-142.

Durrant M, Boyer J, Zhou W, Baldwin IT, Xu S. 2017. Evidence of an evolutionary hourglass pattern in herbivory-induced transcriptomic responses. *New Phytol.* 215:1264-1273.

Dunn CW, Hejnol A, Matus DQ, Pang K, Browne WE, Smith SA, Seaver E, Rouse GW, Obst M, Edgecombe GD, et al. 2008. Broad phylogenomic sampling improves resolution of the animal tree of life. *Nature*. 452:745.

Gerstein MB, Rozowsky J, Yan KK, Wang D, Cheng C, Brown JB, Davis CA, Hillier L, Sisu C, Li JJ, et al. 2014. Comparative analysis of the transcriptome across distant species. *Nature*. 512:445.

Giribet G, Distel DL, Polz M, Sterrer W, Wheeler WC. 2000. Triploblastic relationships with emphasis on the acoelomates and the position of Gnathostomulida, Cycliophora,

497 Plathelminthes, and Chaetognatha: a combined approach of 18S rDNA sequences and
498 morphology. *Syst Biol.* 49:539-562.

499 Goldman N, Yang Z. 1994. A codon-based model of nucleotide substitution for protein-
500 coding DNA sequences. *Mol Biol Evol.* 11:725-736.

501 Gómez-Chiarri M, Warren WC, Guo X, Proestou D. 2015. Developing tools for the study
502 of molluscan immunity: the sequencing of the genome of the eastern oyster, Crassostrea
503 virginica. *Fish Shellfish Immun.* 46:2-4.

504 Hall BK. 1997. Phylotypic stage or phantom: is there a highly conserved embryonic stage
505 in vertebrates?. *Trends Ecol Evol*. 12:461-463.

506 Hejnol A. 2010. A twist in time—the evolution of spiral cleavage in the light of animal
507 phylogeny. *Integr Comp Biol.* 50:695-706.

508 Hu H, Uesaka M, Guo S, Shimai K, Lu TM, Li F, Fujimoto S, Ishikawa M, Liu S, Sasagawa
509 Y, et al. 2017. Constrained vertebrate evolution by pleiotropic genes. *Nat Ecol Evol.* 1:1722.

510 Irie N, Kuratani S. 2011. Comparative transcriptome analysis reveals vertebrate phylotypic
511 period during organogenesis. *Nat Commun.* 2:248.

512 Irie N, Kuratani S. 2014. The developmental hourglass model: a predictor of the basic body
513 plan?. *Development.* 141:4649-4655.

514 Irie N. 2017. Remaining questions related to the hourglass model in vertebrate evolution.
515 *Curr Opin Genet Dev.* 45:103-107.

516 Kalinka AT, Varga KM, Gerrard DT, Preibisch S, Corcoran DL, Jarrells J, Ohler U,
517 Bergman CM, Tomancak P. 2010. Gene expression divergence recapitulates the
518 developmental hourglass model. *Nature.* 468:811.

519 Kalinka AT, Tomancak P. 2012. The evolution of early animal embryos: conservation or
520 divergence?. *Trends Ecol Evol.* 27:385-393.

521 Lambert JD. 2008. Mesoderm in spiralians: the organizer and the 4d cell. *J Exp Zool B*
522 *Mol Dev Evol*. 310:15-23.

Lambert JD. 2010. Developmental patterns in spiralian embryos. *Curr Biol.* 20:R72-R77.

Laumer CE, Bekkouche N, Kerbl A, Goetz F, Neves RC, Sørensen MV, Kristensen RM, Hejnol A, Dunn CW, Giribet G, et al. 2015. Spiralian phylogeny informs the evolution of microscopic lineages. *Curr Biol.* 25:2000-2006.

Levin, M., Anavy, L., Cole, A.G., Winter, E., Mostov, N., Khair, S., Senderovich, N., Kovalev, E., Silver, D.H., Feder, M. and Fernandez-Valverde, S.L., 2016. The mid-developmental transition and the evolution of animal body plans. *Nature.* 531:637-641.

Li WH. 1993. Unbiased estimation of the rates of synonymous and nonsynonymous substitution. *J Mol Evol*. 36:96-99.

Liu J, Robinson-Rechavi M. 2018. Adaptive evolution of animal proteins over development: support for the Darwin selection opportunity hypothesis of Evo-Devo. *Mol Biol Evol.* 35:2862-2872.

Maslakova SA, Martindale MQ, Norenburg JL. 2004. Vestigial prototroch in a basal nemertean, Carinoma tremaphoros (Nemertea; Palaeonemertea). *Evol Dev.* 6:219-226.

Moyers BA, Zhang J. 2015. Phylostratigraphic bias creates spurious patterns of genome evolution. *Mol Biol Evol.* 32:258-267.

Moyers BA, Zhang J. 2017. Further simulations and analyses demonstrate open problems of phylostratigraphy. *Genome Biol Evol.* 9:1519-1527.

Moyers BA, Zhang J. 2018. Toward reducing phylostratigraphic errors and biases. *Genome Biol Evol*. 10:2037-2048.

Nei M, Gojobori T. 1986. Simple methods for estimating the numbers of synonymous and nonsynonymous nucleotide substitutions. *Mol Biol Evol.* 3:418-426.

Nielsen C. 2004. Trochophora larvae: cell-lineages, ciliary bands, and body regions. 1. Annelida and Mollusca. *J Exp Zool B Mol Dev Evol*. 302:35-68.

Nielsen C. 2005. Trochophora larvae: cell-lineages, ciliary bands and body regions. 2. Other groups and general discussion. *J Exp Zool B Mol Dev Evol.* 304:401-447.

549 Pamilo P, Bianchi NO. 1993. Evolution of the Zfx and Zfy genes: rates and interdependence
550 between the genes. *Mol Biol Evol.* 10:271-281.

551 Paps J, Xu F, Zhang G, Holland PW. 2015. Reinforcing the egg-timer: Recruitment of novel
552 Lophotrochozoa homeobox genes to early and late development in the Pacific oyster.
553 *Genome biology and evolution.* 7:677-88.

554 Piasecka B, Lichocki P, Moretti S, Bergmann S, Robinson-Rechavi M. 2013. The hourglass
555 and the early conservation models—co-existing patterns of developmental constraints in
556 vertebrates. *PLoS genetics.* 9:e1003476.

557 Quint M, Drost HG, Gabel A, Ullrich KK, Bönn M, Grosse I. 2012. A transcriptomic
558 hourglass in plant embryogenesis. *Nature* 490:98.

559 Raff RA. 1996. The Shape of Life: Genes. Development, and the Evolution of Animal Form:
560 University of Chicago Press.

561 Raff RA. 2008. Origins of the other metazoan body plans: the evolution of larval forms.
562 *Philos Trans R Soc Lond B Biol Sci.* 363:1473-1479.

563 Richardson MK. 1995. Heterochrony and the phylotypic period. *Dev Biol.* 172:412-421.

564 Richardson MK, Hanken J, Gooneratne ML, Pieau C, Raynaud A, Selwood L, Wright GM.
565 1997. There is no highly conserved embryonic stage in the vertebrates: implications for
566 current theories of evolution and development. *Anat Embryol.* 196:91-106.

567 Sander K. 1983. The evolution of patterning mechanisms: gleanings from insect
568 embryogenesis. *Dev Evol.*

569 Schleip W. 1929. Determination der Primitiventwicklung, ein zusammenfassende
570 Darstellung der Ergebnisse über das Determinationsgeschehen in den ersten
571 Entwicklungsstadien der Tiere.

572 Shigeno S, Takenori S, Boletzky SV. 2010. The origins of cephalopod body plans: a
573 geometrical and developmental basis for the evolution of vertebrate-like organ systems.
574 Cephalopods-Present and Past. 1:23-34.

575 Slack, J. M. W. in Keywords and Concepts in Evolutionary Developmental Biology (eds
576 Hall, B. K. & Olson, W. M.) 2003. Harvard Univ. Press. 476.

577 Slack JMW, Holland PWH, Graham CF. 1993. The zootype and the phylotypic stage.
578 *Nature.* 361:490-492.

579 Uchida Y, Uesaka M, Yamamoto T, Takeda H, Irie N. 2018. Embryonic lethality is not
580 sufficient to explain hourglass-like conservation of vertebrate embryos. *EvoDevo.* 9:7.

581 Baer V, Ernst K. 1828. Über Entwickelungsgeschichte der Thiere: Beobachtung und
582 Reflexion. Vol. 1. Bornträger,.

583 Vellutini BC, Martín-Durán JM, Hejnol A. 2017. Cleavage modification did not alter
584 blastomere fates during bryozoan evolution. *BMC Biol.* 15:33.

585 Wagner, G.P., Kin, K. and Lynch, V.J., 2012. Measurement of mRNA abundance using
586 RNA-seq data: RPKM measure is inconsistent among samples. *Theory in*
587 *biosciences,* 131(4):281-285.

588 Wilson EB. 1904. Experimental studies in germinal localization. II. Experiments on the
589 cleavage-mosaic in Patella and Dentalium. *J Exp Zool.* 1:197–268.

590 Xu F, Domazet-Lošo T, Fan D, Dunwell TL, Li L, Fang X, Zhang G. 2016. High expression
591 of new genes in trochophore enlightening the ontogeny and evolution of trochozoans. *Sci*
592 *Rep*. 6:34664.

593 Yanai I, Peshkin L, Jorgensen P, Kirschner MW. 2011. Mapping gene expression in two
594 Xenopus species: evolutionary constraints and developmental flexibility. *Dev Cell.* 20:483-
595 496.

596 Yang Z. 2014. Molecular evolution: a statistical approach. Oxford University Press.

597 Yin H, Li M, Xia L, He C, Zhang Z. 2018. Computational determination of gene age and
598 characterization of evolutionary dynamics in human. *Brief Bioinform.*

599 Zalts H, Yanai I. 2017. Developmental constraints shape the evolution of the nematode
600 mid-developmental transition. *Nat Ecol Evol.* 1(5). p.0113.

601 Zhang G, Fang X, Guo X, Li L, Luo R, Xu F, Yang P, Zhang L, Wang X, Qi H, et al.
602 2012. The oyster genome reveals stress adaptation and complexity of shell formation.
603 *Nature.* 490:49.

604 Zhang Z, Li J, Yu J. 2006. Computing Ka and Ks with a consideration of unequal
605 transitional substitutions. *BMC Evol Biol.* 6:44.

606

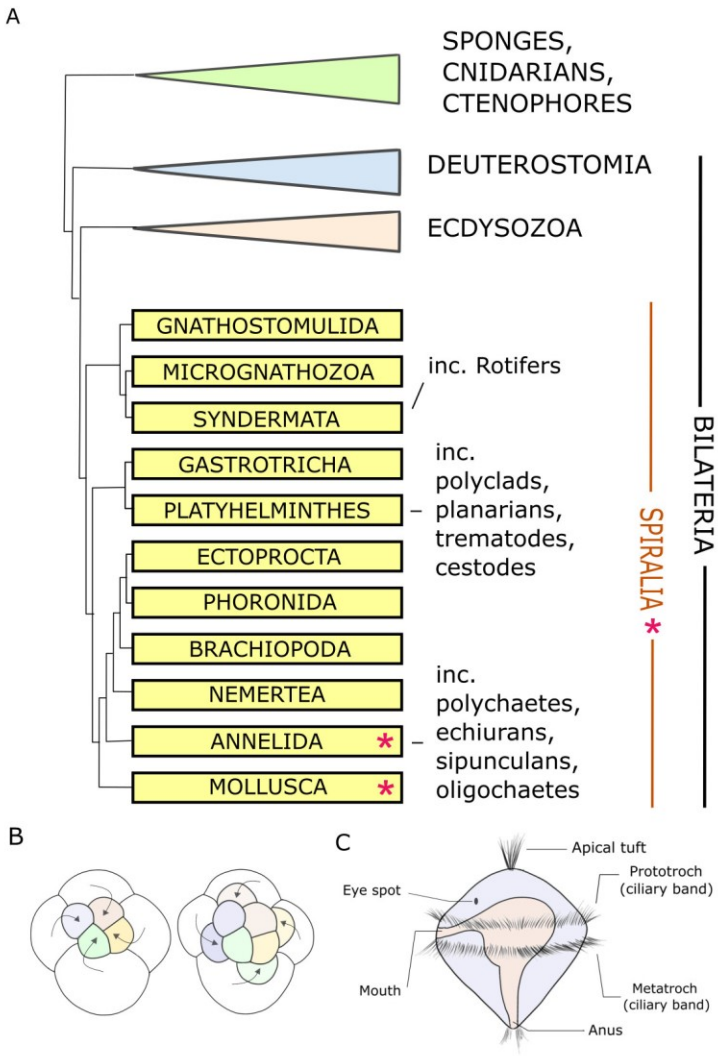

607

608 **Figure 1**: The Spiralia. A: The clade Spiralia within the metazoan phylogeny (based on
609 Laumer et al. 2015). This study examines two molluscs and one polychaete annelid
610 (indicated with "*"). Most previous studies examined taxa in the Deuterostomia and
611 Ecdysozoa clades. B: Spiral cleavage shown in an 8 cell and 16 cell embryo, showing
612 daughter cell asymmetry and the alternating angles of division that characterize this mode
613 of development. The animal pole is up. Homologous spiral cleavage is recognized in
614 molluscs, annelids, nemerteans and platyhelminth flatworms. C: Generalized morphology
615 of trochophore larva, a free-swimming planktonic larva with bands of cilia for
616 locomotion and feeding. Homologous trochophore larvae are recognized in the molluscs
617 and annelids, and this has been proposed to be the phylotypic stage in these groups (see
618 text).

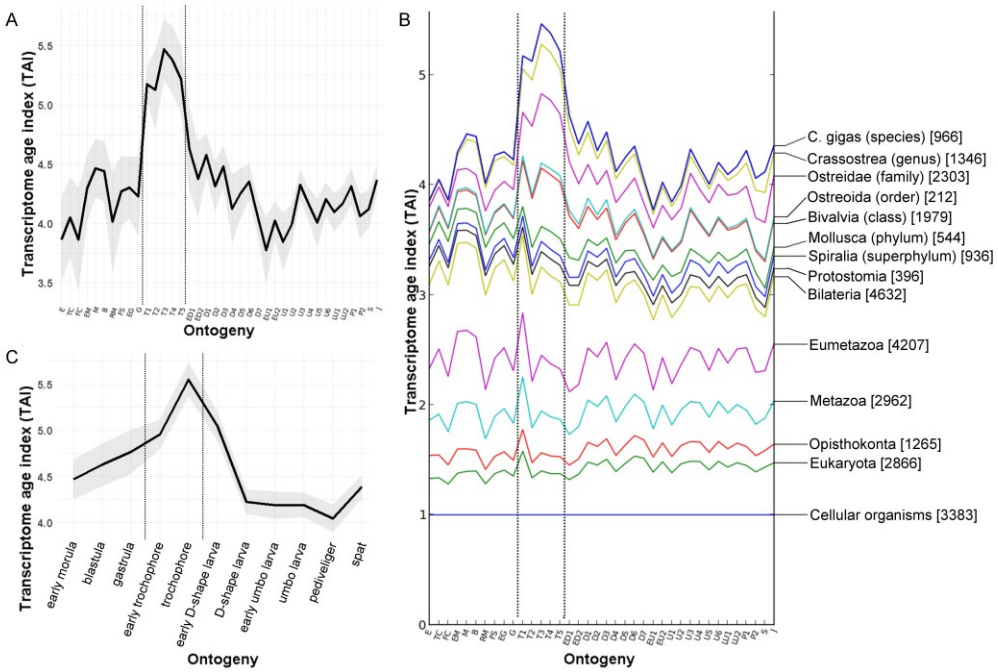

Figure 2: Phylotranscriptomic study of *C. gigas*. Trochophore stages are indicated with dashed lines. A: The TAI profiles of *C. gigas* development showing a reverse hourglass pattern with the highest TAI in the mid-embryonic stage. The shaded area represents the standard deviation estimated by permutation analysis. The hourglass pattern observed in other studies would be relatively higher at early and late stages, and lower at some mid-embryonic stage, for instance the trochophore. B: The TAI profiles of *C. gigas* after removing genes younger than indicated phylostratum cut offs; i.e. the TAI profile labelled "Metazoa" is computed with genes younger than the Metazoa phylostrata removed from the analysis. The number of genes assigned to each phylostrata is shown within brackets. C: The TAI profile of *C. gigas* development using an experimental replicate dataset. The reverse hourglass patterns are significant, as measured by permutation tests (For A, $P = 5.3 \times 10^{-14}$; for C, $P = 3.1 \times 10^{-7}$). The standard deviation and significance test results of B are shown in Fig. S2. Abbreviations: TC: two cell, FC: four cell, EM: early morula stage, M: morula stage, B: blastula stage, RM: rotary movement, FS: free swimming, EG: early gastrula stage, G: gastrula stage, T: trochophore, ED: early D-shaped larva, D: D-shaped larva, EU: early umbo larva, U: umbo larva, LU: later umbo larva, P: pediveliger competent for metamorphosis, S: spat, J: juvenile.

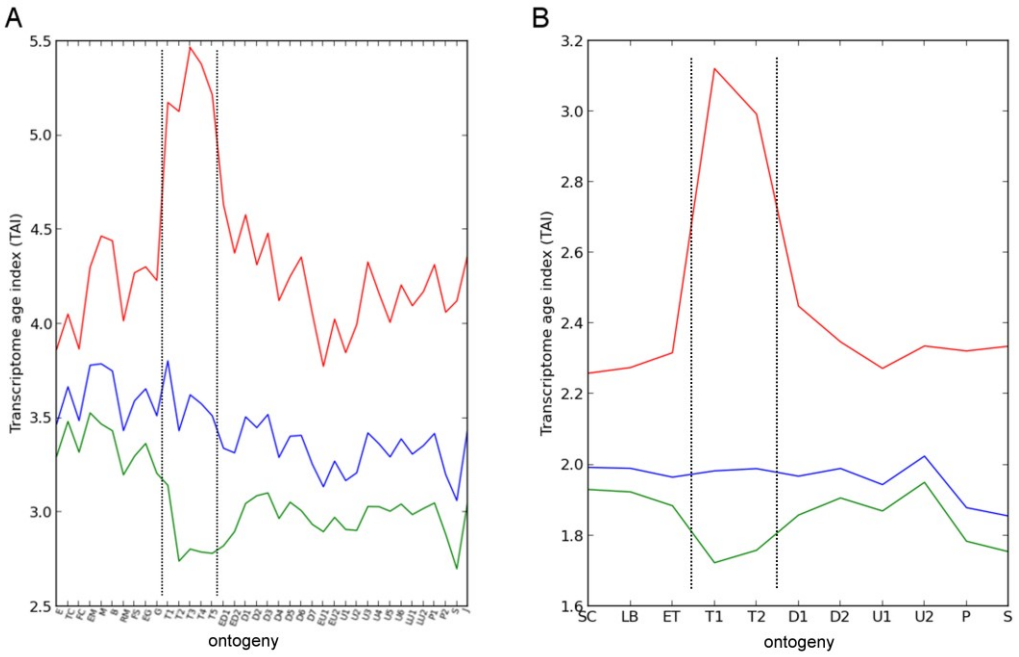

Figure 3: The TAI profiles of *C. gigas* after removing phylostrata younger than Mollusca, using two different calculation methods applied to the same expression dataset (Zhang et al. 2012). Trochophore stages are indicated with dashed lines. A: TAI profiles based on phylostrata assignment and gene expression analysis in this study, using data from Zhang et al. (2012). B: TAI profiles based on phylostrata assignment and gene expression analysis from Xu et al. (2016), using expression data from Zhang et al. (2012). There are fewer timepoints than in A because they used a subset of the stages in Zhang et al. (2012). In both panels: the top line is the TAI profile using all phylostrata; the middle line is the TAI profile after removing phylostrata younger than Mollusca calculated by the method used in this study; and the bottom line is the TAI profile after removing phylostrata younger than Mollusca, calculated by the method used by previous studies, including Xu et al. (2016). Abbreviations follow those in Fig. 2.

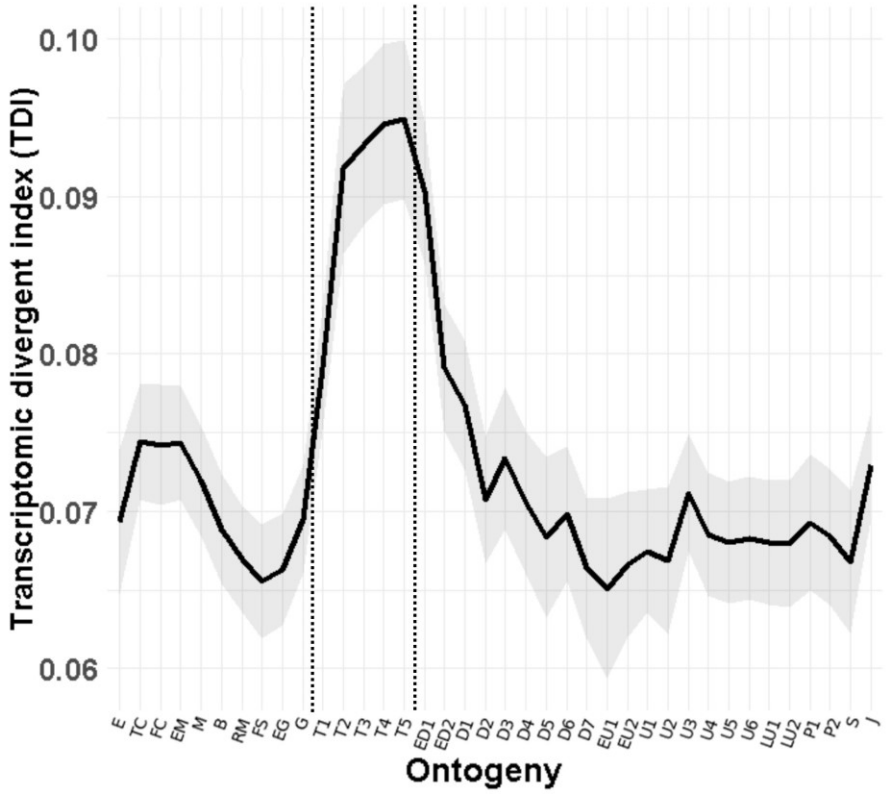

651

652 **Figure 4:** The TDI profiles of *C. gigas* development. Trochophore stages are indicated with
653 dashed lines. The shaded area represents the standard deviation estimated by permutation
654 analysis. The reverse hourglass pattern is significant, as measured by permutation tests
655 ($P = 2.7 \times 10^{-7}$). Abbreviations are the same as Fig. 2.

656

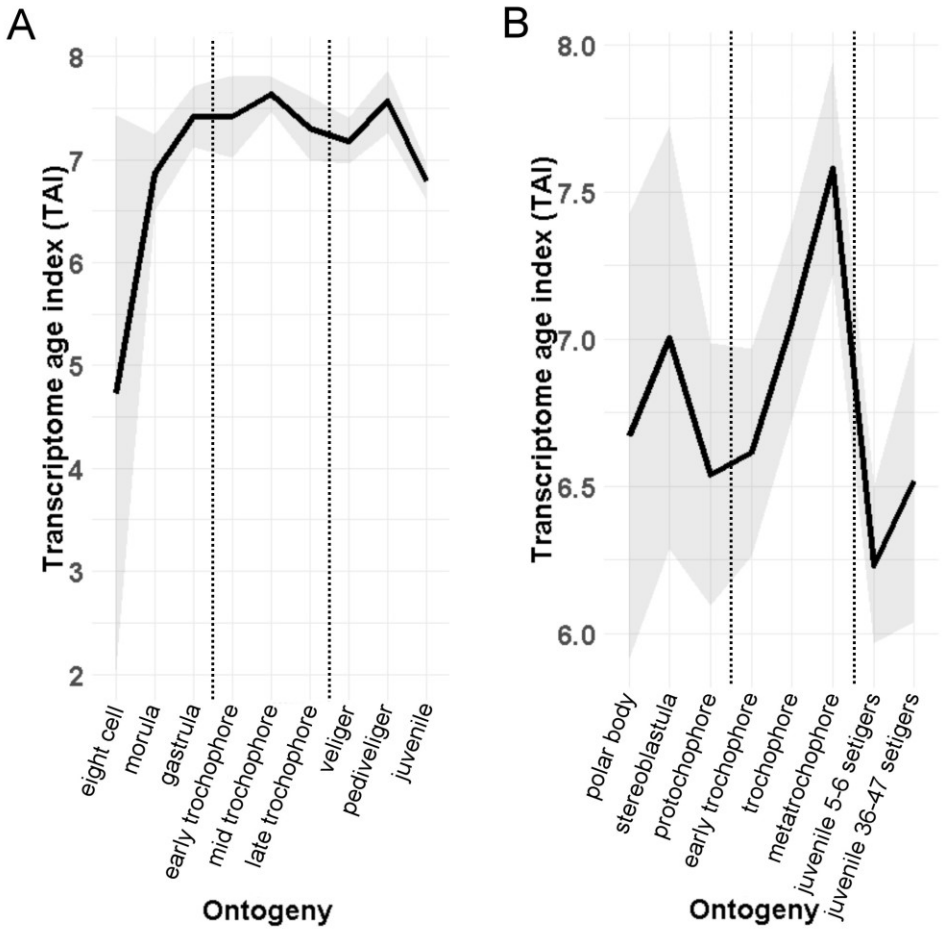

657

658 **Figure 5.** TAI profile of *H. discus hannai* (A) and *P. aibuhitensis* (B). Both have their
659 highest TAI in one of the trochophore stages. Trochophore stages are indicated with dashed
660 lines. The shaded area represents the standard deviation estimated by permutation analysis.
661 The reverse hourglass patterns are significant, as measured by permutation tests (For A,
662 P = 0.019; for B, P = 0.026).